

FASHIONABLY LATE? BUILDING UP THE MILKY WAY'S INNER HALO

HEATHER L. MORRISON

Department of Astronomy, Case Western Reserve University, Cleveland, OH 44106

AMINA HELMI

Kapteyn Astronomical Institute, University of Groningen, PO Box 800, 9700 AV Groningen, the Netherlands

JIAYANG SUN, PENG LIU AND RONGFANG GU

Department of Statistics, Case Western Reserve University, Cleveland, OH, 44106

JOHN E. NORRIS

Research School of Astronomy and Astrophysics, The Australian National University, Mt Stromlo Observatory, Cotter Road, Weston ACT 2611, Australia

PAUL HARDING

Department of Astronomy, Case Western Reserve University, Cleveland, OH 44106

T.D. KINMAN

National Optical Astronomy Observatories, PO Box 26732, Tucson AZ 85726

AMANDA A. KEPLEY*

Department of Astronomy, University of Wisconsin–Madison, 475 North Charter Street, Madison, WI 53706

KENNETH C. FREEMAN

Research School of Astronomy and Astrophysics, The Australian National University, Mt Stromlo Observatory, Cotter Road, Weston ACT 2611, Australia

MARY WILLIAMS

Research School of Astronomy and Astrophysics, The Australian National University, Mt Stromlo Observatory, Cotter Road, Weston ACT 2611, Australia and Astrophysikalisches Institut Potsdam, An der Sternwarte 16, D-14482 Potsdam, Germany

JEFFREY VAN DUYN

Department of Astronomy, Yale University, P.O. Box 208121, New Haven, CT 06520

Draft version December 12, 2008

ABSTRACT

Using a sample of 246 metal-poor stars (RR Lyraes, red giants and RHB stars) which is remarkable for the accuracy of its 6-D kinematical data, we find, by examining the distribution of stellar orbital angular momenta, a new component for the local halo which has an axial ratio $c/a \sim 0.2$, a similar flattening to the thick disk. It has a small prograde rotation but is supported by velocity anisotropy, and contains more intermediate-metallicity stars (with $-1.5 < [\text{Fe}/\text{H}] < -1.0$) than the rest of our sample. We suggest that this component was formed quite late, during or after the formation of the disk. It formed either from the gas that was accreted by the last major mergers experienced by the Galaxy, or by dynamical friction of massive infalling satellite(s) with the halo and possibly the stellar disk or thick disk.

The remainder of the halo stars in our sample, which are less closely confined to the disk plane, exhibit a clumpy distribution in energy and angular momentum, suggesting that the early, chaotic conditions under which the inner halo formed were not violent enough to erase the record of their origins. The clumpy structure suggests that a relatively small number of progenitors were responsible for building up the inner halo, in line with theoretical expectations.

We find a difference in mean binding energy between the RR Lyrae variables and the red giants in our sample, suggesting that more of the RR Lyraes in the sample belong to the outer halo, and that the outer halo may be somewhat younger, as first suggested by Searle & Zinn (1978). We also find that the RR Lyrae mean rotation is more negative than the red giants, which is consistent with the recent result of Carollo et al. (2007) that the outer halo has a retrograde rotation and with the difference in kinematics seen between RR Lyraes and BHB stars by Kinman et al. (2007).

Subject headings: Galaxy: halo — Galaxy: formation — Galaxy: evolution — Galaxy: kinematics and dynamics

1. INTRODUCTION: RECONSTRUCTION OF HALO HISTORY

One of the central aims of the study of old populations in the Galaxy is the reconstruction of its history from their properties today. We will begin here by considering the different approaches to modeling the structure of the halo. Searle & Zinn (1978) took an important first step toward our current understanding of the hierarchical build-up of galaxies when they noted that “the loosely bound clusters of the outer halo have a broader range of age than the more tightly bound clusters.” Perhaps because of our taxonomic heritage, subsequent stellar populations workers have tended to describe the complex structure of the stellar halo in terms of two components. For example, in one of the first attempts at “Armchair Cartography” (the use of a local sample of halo stars to reconstruct the halo density distribution) Sommer-Larsen & Zhen (1990) inferred a two-component halo, with one component quite flattened. However, the study was limited by the small sample and the relatively inaccurate distances and velocities then available.

More global studies of the halo using kinematically unbiased samples also found variants on this two-component halo. Kinman et al. (1965) and Hartwick (1987) used RR Lyrae variables to show that the flattened component dominates in the inner halo, and the spherical component in the outer halo. Preston et al. (1991) and Kinman et al. (1994) found a similar spatial distribution using blue horizontal branch stars and RR Lyraes. Chiba & Beers (2000) used a larger, local sample and confirmed the results of previous studies. Most recently, Carollo et al. (2007) used more than 20,000 local stars from SDSS to further quantify this “halo dichotomy”. They find that the outer halo is significantly more metal-poor than the inner halo, and has a retrograde mean rotation.

The influential work of Zinn (1993) (building on the earlier work of Searle & Zinn 1978) developed the two-component halo idea further, using globular cluster kinematics. Zinn subdivided the halo globular clusters into different groups using horizontal branch morphology (as a proxy for age) and found different spatial distributions and kinematics for the two groups. The Old Halo clusters in the inner halo show a flattened distribution and have prograde rotation (although much less than the disk’s). The Younger Halo is spherical and has no net rotation.

With the exception of the work of Sommer-Larsen & Zhen (1990) and Chiba & Beers (2000), all of the works which derived a flattened inner halo were based on samples of stars more distant than ~ 1 kpc. However, Preston et al. (1991) noted a curious anomaly: when they used their density model (including an inner halo with $c/a=0.7$ at the Sun) to predict the density of RR Lyraes in the solar neighborhood, the model predictions fell seriously short: by a factor of at

least two, even though the local sample is unlikely to be complete at very low latitudes. Preston et al. followed this fact to its logical conclusion and suggested that the halo has an additional highly flattened component found only very close to the plane. This paper will confirm the detection of the highly flattened halo component with a new sample of halo stars which have a median distance of 1 kpc.

How can we explain these results in the context of current models of galaxy formation? There have been significant advances in recent years which have developed a more nuanced picture of galaxy formation in a number of areas. The concept which has changed least over the years is that of disk formation: a smooth, dissipational collapse which conserves the angular momentum of the infalling material seems the only way to produce large galaxy disks like our own. Halo formation was likely much messier. Our concepts here have changed more with time, as the hierarchical paradigm for structure formation has permeated the field: we now understand that accretion is fundamental to the formation of the dark halo. Classical expectations are that this accretion is violent in its early stages: the rapid variations in the gravitational potential caused by early mergers should smooth out any record of the discrete origins of early halo stars. We will see below that this is not entirely correct.

Before the disk forms, halo stars could be produced by the mergers of gas-rich objects (the “dissipative mergers” of Bekki & Chiba 2001). (Only minor accretions can occur after the present-day disk forms, because otherwise the fragile kinematically cold disk would be destroyed). The stellar halo can also be built up by accretions of larger objects, helped by dynamical friction (which was likely the way the progenitor of the globular cluster ω Centauri arrived in the inner halo), or by the simpler accretion of smaller satellites which did not feel dynamical friction. We will see that there are opportunities for all of these processes to build up a flattened inner halo.

The use of integrals such as energy and angular momentum, which are conserved under some conditions as the Galaxy evolves, can be a powerful tool for tracing the Galaxy’s history. For example, Lynden-Bell & Lynden-Bell (1995) and Johnston et al. (1996) showed how energy can be used to identify stars with common origins, and Helmi et al. (1999), Helmi & de Zeeuw (2000), Chiba & Beers (2000) and Helmi et al. (2006) considered different components of angular momentum and energy. Helmi et al. (1999) illustrate the different information available from study of stellar velocities and of angular momenta: their Figure 2 shows that the debris from a disrupting satellite is all found in the same place in the angular momentum diagram, but that different streams from this satellite may be seen with distinct velocities (moving towards and away from the plane, for example).

In this paper we analyse a sample of metal-poor stars from the solar neighborhood which is remarkable for the accuracy of its kinematic data. These high-quality data

*Current address: Department of Astronomy, University of Virginia, Charlottesville, VA 22904-4325

have well-determined orbital angular momenta and energies, making them well-suited to the approach using integrals. We find patterns in the distribution of energy and angular momentum, never observed before, which we will relate to different formation and evolution processes. The location of our sample (its stars have a median distance of 1 kpc) influences the processes we can study. The solar neighborhood lies within the inner halo¹ but it is also centered on the disk. We will focus in this paper on processes which either form stars in the inner halo or transfer stars into this region. We will seek to distinguish between stars formed very early in the inner galaxy (its original inhabitants) and the fashionably late arrivals which were accreted later from the outer halo. These could either have orbits sufficiently eccentric to bring them into the inner halo or had their orbits modified by dynamical friction on the parent satellite to move them from the outer to the inner halo.

The plan of this paper is as follows. In Section 2 we describe our sample and investigate the properties of these stars in angular momentum, energy and metallicity; and discuss the trends that we discern. In Section 3 we will relate our results to the work of others, and in Section 4 we will discuss the different formation paths for the inner halo, and how our data constrain them.

2. ANALYSIS OF LOCAL HALO SAMPLE

2.1. *Sample*

Our sample is composed of red giants, red horizontal branch (RHB) stars and RR Lyrae variables with $[\text{Fe}/\text{H}] < -1.0$ and distances less than 2.5 kpc. The red giants and RHB stars are all taken from the sample of well-studied stars in Anthony-Twarog & Twarog (1994), and comprise all the stars in that study with available velocity data. Its RR Lyrae variables include a large number with new, accurate radial velocity measurements (van Duyn et al, in preparation) and a few with velocities from the literature with similar or higher accuracy. The sample contains 246 stars, and can be accessed at <http://astronomy.case.edu/heather/fashlate.sample>.

The sample has a large overlap with the “combined data sample” of Kepley et al. (2007); but we have restored 12 stars which they removed from their sample because they were likely metal-weak thick disk stars, in order to make the sample selection criteria clearer. We removed 22 giant stars which were in the Kepley et al sample but not in the sample of Anthony-Twarog & Twarog (1994), as they have distances of significantly lower quality. We have also added a few giants from Anthony-Twarog & Twarog (1994) which were not in the Kepley et al sample because they had radial velocities measured after 2000, and so were not in the catalog of Beers et al. (2000) on which it was based.

Our sample contains stars with accurate distances and well-quantified distance errors, allowing us to calculate errors on derived quantities like energy and angular momentum via a Monte-Carlo procedure. There is a full description of our distance error calculation (which used a Monte-Carlo procedure to take account of all the different contributing errors) in Section 2.2.3 of Kepley et al.

(2007). We emphasise the importance of our small distance errors here: energy and angular momentum are strongly dependent on distance errors since two out of three components of velocity are obtained by multiplying the proper motion by the distance.

Except for the three stars with new velocities, our sample is a subset of the compilation of halo stars of Beers et al. (2000). We have improved the data in several ways. First, we removed the effect of the large distance errors in the sample found by Kepley et al. (2007) by limiting the giants and RHB stars in our sample to those with very well-defined luminosities and metallicities, by using only those from the sample of Anthony-Twarog & Twarog (1994). The Beers et al. (2000) sample contains 736 stars with $[\text{Fe}/\text{H}] < -1.0$ and distances less than 2.5 kpc which have proper motion measurements. 435 of these stars are red giants, RHB stars or RR Lyrae variables. We estimate that 60% of these stars have the well-determined distances and well-quantified distance errors that are required for our study; the other 40% have data of significantly lower quality, either because of the lack of a luminosity measurement which separates stars below the horizontal branch from those on the horizontal branch, or because the metallicity measurements are less accurate and not on a consistent scale. However, RR Lyrae variables have large pulsational velocity amplitudes and so require significant effort to constrain their systemic velocities; many of the RR Lyraes in Beers et al. (2000) have large errors on their velocities. The restriction of our sample to those with both good distance and velocity measurements cuts the sample down to 246 stars². It has a median distance of 1 kpc and a median distance error of 7% (error estimates for red giant and RHB distances are given in Table 1 of Kepley et al. 2007).

Since our giant and RHB sample is selected on metallicity only, and the RR Lyrae variables are selected via their variability, we have no kinematic selection effects in the sample. RR Lyraes are generally thought to be very old, while the giants and RHB stars could possibly have a larger range of age, including both younger and older objects. The RR Lyrae sample has a somewhat higher median metallicity than the giant and RHB sample because the latter was identified with objective-prism searches which tend to favor extremely weak-lined stars.

2.2. *Angular Momentum plots*

Helmi et al. (1999) used the angular momentum components L_z and L_\perp to show that around 10% of local halo stars were formed via destruction of a satellite whose debris now occupies the inner halo. They compared the amount of rotation of a given star’s orbit (L_z) to L_\perp , which combines the other two components of angular momentum ($L_\perp = \sqrt{(L_x^2 + L_y^2)}$)³. For a local sample, L_\perp is dominated by v_z , the velocity perpendicular to the plane, since y and z are close to zero, while x is around 8 kpc. Figure 1 shows this clearly. Thus the L_z, L_\perp dia-

¹ Contrast the Sun’s R_{gc} of 8 kpc with distant halo stars at more than 100 kpc (Clewley et al. 2005)

² We have discarded one star, HD220127, which has large errors on its derived velocities using the distance from Anthony-Twarog & Twarog (1994) and a significantly different distance in Schuster et al. (2006).

³ $L_x = yv_z - zv_y$; $L_y = zv_x - xv_z$; $L_z = xv_y - yv_x$; see the Appendix of Kepley et al. (2007) for a detailed discussion of our coordinate system.

gram is similar to the v_ϕ vs v_z diagrams which contrast rotational angular momentum with the vertical extent of an orbit. Stars with L_z less than zero are on retrograde orbits.

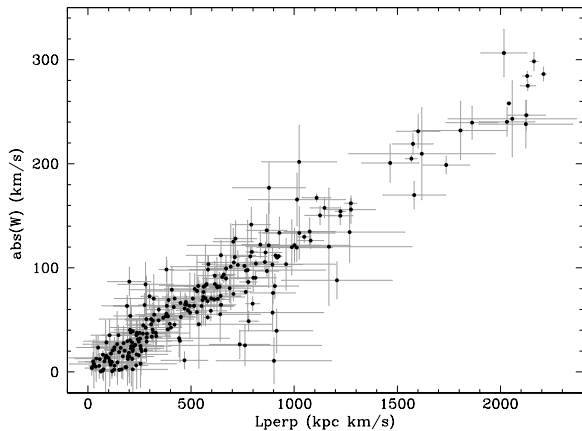


FIG. 1.— Plot of angular momentum L_\perp vs the absolute value of the star's W velocity.

Figure 2 shows the distribution of stars in our sample in L_z and L_\perp . To show the location of stars with near-circular orbits which never reach far from the plane, the stars from the Nordström et al. (2004) sample, a magnitude-limited sample of stars with distances up to ~ 200 pc, are shown in grey on the same diagram. The Nordström et al. sample is almost completely dominated by thin disk stars. As expected for a sample of stars in the thin disk whose orbits are confined to the plane, few of these stars have L_\perp greater than 200 kpc km s $^{-1}$, and their L_z values are higher than almost all stars in our halo sample.

Kepley et al. (2007) have discussed star streams in the sample: outliers such as the Helmi et al. (1999) group near $(L_z, L_\perp) = (1000, 2000)$ kpc km s $^{-1}$ and the very retrograde stars with (L_z, L_\perp) near $(-2000, 1500)$ kpc km s $^{-1}$. In this paper we focus, not on these outliers, but on the majority of the stars in the sample which occupy the region normally described as the smooth, well-mixed halo. Thus, for the rest of the paper, we consider stars with $L_\perp < 1400$ kpc km s $^{-1}$. Figure 3 shows a contour plot of the stellar density in this diagram.

The classical description of halo kinematics uses a velocity ellipsoid (Schwarzschild 1907) with independent Gaussian distributions in v_x, v_y and v_z . In the small range of distance in our sample (recall that the median distance is 1 kpc) these assumptions will lead to roughly Gaussian distributions of L_z and L_\perp as well. It is clear from Figure 2 that such a velocity ellipsoid is not a good description of our sample, even when outliers are removed by restricting it to stars with $L_\perp < 1400$ kpc km s $^{-1}$. The only part of the sample that appears smooth and close to Gaussian is the region occupied by stars whose orbits are quite confined to the plane: those with low L_\perp ($\lesssim 400$ kpc km s $^{-1}$). This is the region of L_\perp occupied by disk and thick disk stars in Figure 2. For values of L_\perp above 400 kpc km s $^{-1}$, the distribution looks quite clumpy. For example, there is a pronounced gap around $(L_z, L_\perp) = (500, 400)$ kpc km s $^{-1}$ and clumps at

(750, 500) and (0, 900) kpc km s $^{-1}$.

2.3. Statistical Analysis

We use two statistical approaches to quantify the structure in the (L_z, L_\perp) diagram. In the first approach, which we present here in detail, we fit mixtures of Gaussian distributions to L_z distributions for different ranges of L_\perp , decide how many components are needed in each L_\perp range (based on statistical model selection procedures), and then estimate the value of L_\perp where the distributions change character. Then we compare the results of the first mixture fits with those based on the actual estimated “change points” (the values of L_\perp where the distributions change character).

We begin by dividing the sample by eye into three ranges of L_\perp : (0–350, 350–700, 700–1400) and determining whether each distribution of L_z is best described by a single Gaussian:

$$f \sim N(\mu, \sigma^2)$$

or a mixture of two:

$$f \sim pN(\mu_1, \sigma_1^2) + (1-p)N(\mu_2, \sigma_2^2), 0 < p < 1$$

Figure 4 shows the three histograms. It can be seen that the histogram for the lowest L_\perp values (stars whose orbits are confined to the disk plane) looks unimodal, while the other two (stars with orbits which reach further from the plane) appear less so.

We decided whether to use a unimodal or bimodal model using an extension to the standard procedure of calculating the likelihood of the sample under a given model, the Akaike Information Criterion (Akaike 1974, AIC hereafter):

$$AIC = -2 \log L(\hat{\theta}) + 2d$$

Here $L(\hat{\theta})$ is the likelihood function for the model with parameters θ and d is the number of parameters in a competing model, unimodal or bimodal. A model with one extra parameter is thus penalized by the factor of d when comparing values of $\log(\text{likelihood})$.

Model comparisons using the AIC can be seen in Table 1, where the preferred models are shown in bold face. A competitive model selection criterion is Schwarz' Bayesian Information Criterion (BIC, Schwarz 1978) which changes $2d$ to $\log(n)d$, where n is the number of data points. If we had used the BIC for the $L_\perp = 0 - 350$ range, it would have favored the one-component model even more strongly, because this range of L_\perp contains the largest number of stars. However, Ishwaran et al. (2001) have demonstrated that AIC is a better criterion for comparison of mixture models, so we prefer to use this for our analysis. It should be noted that although the difference between the AIC values for one and two components looks small compared to its large value, a difference of 2 in its numerical value is equivalent to the amount which justifies an additional parameter; also, different analyses discussed below give similar results.

We have shown that when we divide the sample into three L_\perp ranges by eye, we find that the stars whose orbits are confined near the plane have a different distribution than those whose orbits reach further from the

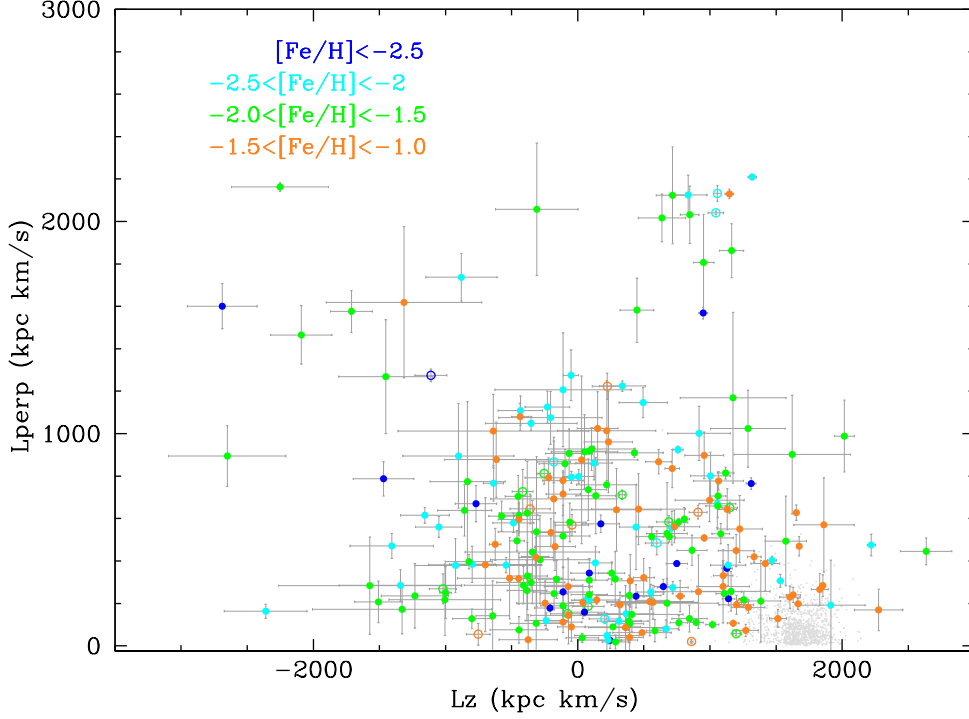


FIG. 2.— Plot of angular momenta L_z (measuring rotation) vs L_\perp (in our sample, this correlates with the distance a star's orbit reaches from the disk plane) for stars with $[\text{Fe}/\text{H}] \leq -1$. It can be seen that the errors on these quantities are quite small for most of the sample. RHB stars are plotted with open circles. Stars from Nordström et al. (2004) with $[\text{Fe}/\text{H}] > -1.0$ (which are predominantly from the disk and thick disk) are plotted in grey, and the globular cluster M4 is shown with an open 5-pointed star.

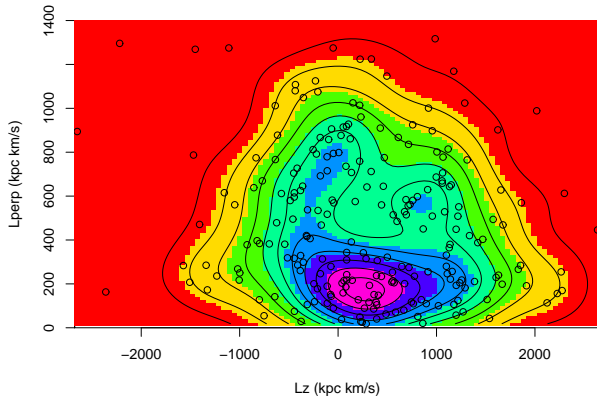


FIG. 3.— Kernel Density Estimate plot of angular momenta L_z vs L_\perp for stars in our sample with $[\text{Fe}/\text{H}] \leq -1.0$.

TABLE 1
MODEL COMPARISON FOR DATA GROUPED IN
 L_\perp BY EYE

L_\perp range	n	AIC(1)	AIC(2)
0–350	103	1685.431	1686.274
350–700	63	1041.645	1035.361
700–1400	61	1018.468	1015.161

plane: the former have a simple Gaussian distribution of L_z , while the latter have a bimodal distribution. We can now remove the effect of our subjective choice of L_\perp

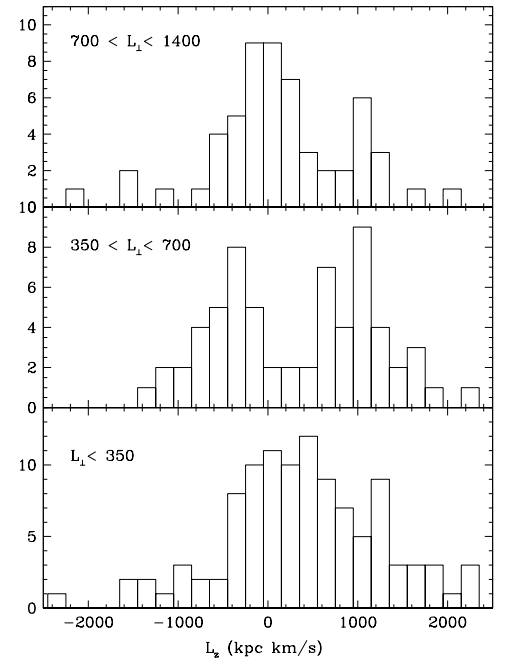


FIG. 4.— Histograms of L_z for stars with $[\text{Fe}/\text{H}] \leq -1.0$, for three ranges of L_\perp as shown.

range using a change point analysis (Csörgö and Horváth 1997, Chen and Gupta 2000, Ganocy 2003), which will solve for the best values of L_\perp to separate the three groups. In particular we are interested in the value of L_\perp where the distribution changes from unimodal to bi-

modal, and in interpreting this number in terms of the Galaxy’s known stellar populations.

For the change point analysis we fit the following model to the data, solving for the two dividing points $L_{\perp,1}$ and $L_{\perp,2}$:

$$f_1(L_z|L_{\perp} < L_{\perp,1}) \sim N(\mu_1, \sigma_1^2)$$

$$f_2(L_z|L_{\perp,1} \leq L_{\perp} < L_{\perp,2}) \sim pN(\mu_2, \sigma_2^2) + (1-p)N(\mu_3, \sigma_3^2)$$

$$f_3(L_z|L_{\perp,2} \leq L_{\perp} < 1400) \sim N(\mu_4, \sigma_4^2)$$

, where $0 < p < 1$.

(We have chosen a single Gaussian for the highest L_{\perp} group to make the change point analysis simpler; note that the middle group has the strongest deviation from Gaussian shape.)

The dividing points which produce the highest likelihood are $(L_{\perp,1}, L_{\perp,2}) = (349, 709)$ kpc km s⁻¹; these are quite close to the original values chosen by eye. Repeating the analysis summarized in Table 1 with these slightly different values produces the same result: the sophisticated AIC criterion prefers a Gaussian distribution for L_{\perp} less than 349 kpc km s⁻¹, and mixtures of two Gaussians for the other two ranges of L_{\perp} .

The lower change point, $L_{\perp} = 349$ kpc km s⁻¹, is particularly interesting because it represents the value of L_{\perp} below which the distribution of L_z is Gaussian. A rough calculation (setting $y = z = 0$ and $x = 8$) shows that this L_{\perp} “change point” corresponds to $|v_z| \sim 40$ km s⁻¹. The z velocity dispersion of all stars in our sample with $L_{\perp} < 350$ kpc km s⁻¹ is 30 km s⁻¹,⁴ intermediate between the thin disk ($\sigma_z = 20$ km s⁻¹) and the thick disk ($\sigma_z = 40$ km s⁻¹).

Table 2 shows the best fit mean and sigma for these models. First, it should be noted that none of the groups have rotational properties at all close to the thin and thick disks’ ($\langle L_z \rangle \sim 1700$ kpc km s⁻¹). The low L_{\perp} group (stars with orbits closely confined to the plane) shows a mild prograde rotation ($\langle L_z \rangle = 364$ kpc km s⁻¹, corresponding roughly to $v_{\phi} = 45$ km s⁻¹). The other two groups (containing stars with orbits reaching further from the plane) have more complex distributions of L_z , as can be seen in Figure 4. L_z is roughly zero in the mean but quite clumpy, making the mean a less informative parameter.

It is important to note here that the somewhat higher mean rotation of the group with orbits very close to the plane is not due to thick disk contamination: Figure 2 shows that there are almost no stars in this lowest L_{\perp} bin in the region occupied by disk and thick disk stars, which have near circular orbits. The low L_{\perp} stars in our sample are on highly eccentric orbits close to the plane, as was first noted by Sommer-Larsen & Zhen (1990). The presence of this low scale height component of the metal poor halo was not found by previous studies, perhaps because of the significantly larger errors or the high-latitude sampling of some surveys which led to a lack of data close to the plane.

⁴ Fortuitously, these two quantities do not vary exactly in lock-step, which would mean that truncating L_{\perp} would produce a truncated distribution in v_z and make estimation of the velocity dispersion difficult.

What is the spatial distribution of these stars with low L_{\perp} ? We cannot measure it directly from our sample, because there were latitude-related selection effects in the initial surveys on which it was based (see Section 3.2 below), and our sample contains only stars from these surveys which have been followed up extremely thoroughly by a number of authors, thus giving very accurate kinematical measurements, rather than all stars identified down to a certain magnitude by the surveys. It is also not possible to simply compare the z velocity dispersion of these stars with that of the thick disk, because the thick disk’s large degree of rotational support adds extra flattening. However, we can make an estimate of the axial ratio of this component using its velocity ellipsoid, and employing the tensor virial theorem. Binney & Tremaine (1987) discuss the case of a self-gravitating population in the context of the flattening and rotation of elliptical galaxies, and Helmi (2008) discusses the case of a tracer population such as the stellar halo. We find that the velocity ellipsoid for stars with L_{\perp} less than 350 kpc km s⁻¹, $(\sigma_U, \sigma_V, \sigma_W) = (144, 111, 30)$, corresponds to a flattening $c/a = 0.2$. This contrasts markedly with the flattening for the entire halo at the solar radius ($c/a = 0.6$), which can either be derived directly from the models of, for example, Preston et al. (1991) or from the local velocity ellipsoid (see Helmi 2008).

In our second statistical analysis, we used the model-based clustering method in the R project for statistical computing⁵ package MCLUST⁶. In the MCLUST analysis, the data are fit by a mixture of a finite number of two-dimensional Gaussian distributions, and the best fit is computed using a modification of the AIC with a second order correction for small sample sizes (AICc⁷). We considered both 2-D Gaussians with major and minor axes parallel to the L_z and L_{\perp} axes, and more complex models where the Gaussians could be oriented in any direction. A good fit was obtained with two elliptical Gaussians. The one at low L_{\perp} is quite flattened, with major axis parallel to the L_z axis; the other, for the higher L_{\perp} values, is a rounder elliptical Gaussian. These Gaussians can be seen in Figure 5. The separation point between the two elliptical Gaussians is close to $L_z = 350$, confirming, with a different analysis technique, the results of the change point analysis reported above. Another analysis, using the AIC only, divided the data with L_{\perp} greater than 350 into five different clusters, so we should not take the two-Gaussian result shown in Figure 5 to indicate a lack of substructure in the data with high L_{\perp} .

2.4. Binding Energy

It will be useful in our discussion of the different processes which deposit stars in the inner halo to consider the total energy of each star, as well as its angular momentum. Figure 6 shows the traditional energy-angular momentum plot. (Note that we have computed these values for the entire sample, not just those stars with L_{\perp} less than 1400 kpc km s⁻¹.) To calculate total energy we have used the Galaxy potential of Johnston et al. (1995) with a somewhat smaller disk mass of $7.5 \times 10^{10} M_{\odot}$ and

⁵ <http://www.r-project.org>

⁶ <http://cran.r-project.org/doc/packages/mclust.pdf>

⁷ http://en.wikipedia.org/wiki/Akaike_information_criterion

TABLE 2
PARAMETERS OF BEST FIT GAUSSIAN MIXTURES
FOR L_z DISTRIBUTIONS FOR DIFFERENT L_\perp
RANGES

L_\perp range	p	μ_1	σ_1	μ_2	σ_2
0–350	1.0	364	848
350–700	0.45	−460	348	1088	567
700–1400	0.70	186	1035	54	194

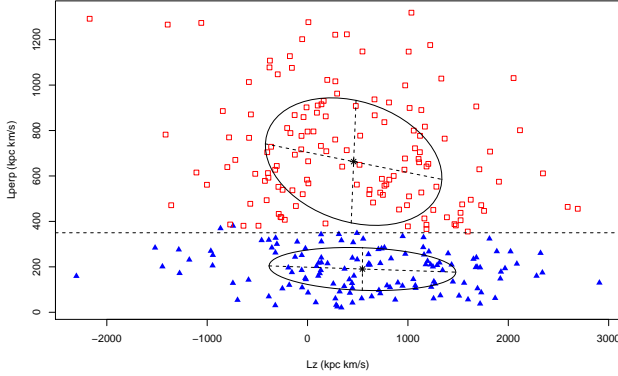


FIG. 5.— MCLUST fit of elliptical Gaussians to our data. It can be seen that this alternative analysis produces very similar answers: a highly flattened elliptical Gaussian for the low values of L_\perp , separated from the other data near $L_\perp = 350$ kpc km s^{-1} .

a dark halo circular velocity of 155 km s^{-1} . We set the potential energy equal to zero at $R=200$ kpc.

It can be seen that the majority of stars in our sample have higher binding energy (lower E_{tot}) than the energy corresponding to the LSR velocity. This is expected in a sample of halo stars because of the halo’s steep density distribution ($R^{-3.5}$, measured for RR Lyraes by Vivas & Zinn 2006). The clumpiness that we see in the L_z, L_\perp diagram is also visible in this diagram, particularly along the lines $L_z=1200$ and 0 kpc km s^{-1} . The clump near $L_z=1100$ kpc km s^{-1} , $E_{tot}=-160,000$ km $^2/s^2$ has energy and angular momentum similar to the Arcurus group (Eggen 1998, Navarro et al. 2004). We also see the “plume” at $L_z \sim -300$ kpc km s^{-1} and a large range of E_{tot} which has been remarked upon by Dinescu (2002) and Brook et al. (2003). They suggested that this “plume” is debris from the progenitor of ω Centauri.

In Figures 7 and 8 we see the intriguing result that the RR Lyraes and red giants in our sample show differences in binding energy⁸. (Note that we have excluded the RHB stars from this comparison for clarity.) The red giants (which have significantly more metal-poor stars) are on average more tightly bound to the Galaxy than the RR Lyraes. We find that 55% of the RR Lyrae sample have binding energy less than the LSR’s, compared with only one third of the red giants. We tested the statistical significance of this result by sampling the (122 star) red giant sample with replacement 1000 times in order to produce samples of the same size as the RR Lyrae sample (99 stars). None of the thousand samples had more than 55% with binding energy less than the LSR’s, and only

⁸ The differences between the two samples in the L_z-L_\perp diagram are much more subtle.

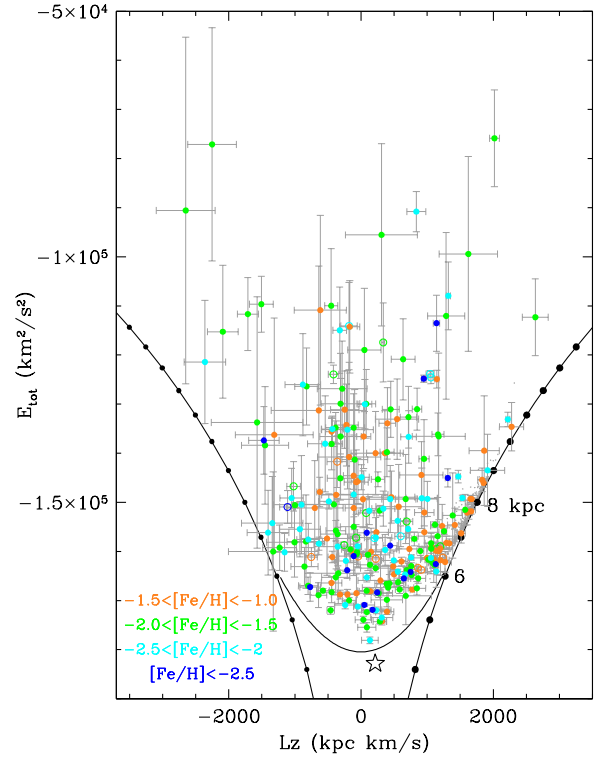


FIG. 6.— The energy-angular momentum diagram for our sample. Points are coded by metallicity as in Figure 2, and the predominantly disk stars from Nordström et al. (2004) are shown in grey. RHB stars are again plotted with open circles. Black lines with closed circles show the circular orbits at a given position, with orbits at 6 and 8 kpc marked, while the parabola at the bottom shows the position of orbits in the plane with apogalacticon 7 kpc. The star is the globular cluster M4, which has a near-radial orbit and is currently 6.3 kpc from the galactic center.

one had half the sample with less binding energy than the LSR. It is clear that the giants and the RR Lyrae variables have different distributions in binding energy. We note that since less than 10% of our sample are RHB stars, it is not possible to make a similar check for these stars.

This result is a kinematic counterpart of the Preston et al. (1991) result that RR Lyraes and BHB stars have different spatial distributions, with the RR Lyraes less centrally concentrated than the BHB stars. It is also related to the different population properties of both field RR Lyraes and globular clusters when they are divided according to the Oosterhoff dichotomy (eg Lee & Carney 1999, Miceli et al. 2008) which is likely related to age (Lee & Carney 1999, Jurcsik et al. 2003).

The giants in our sample will evolve onto the horizontal branch as they age, and since the horizontal

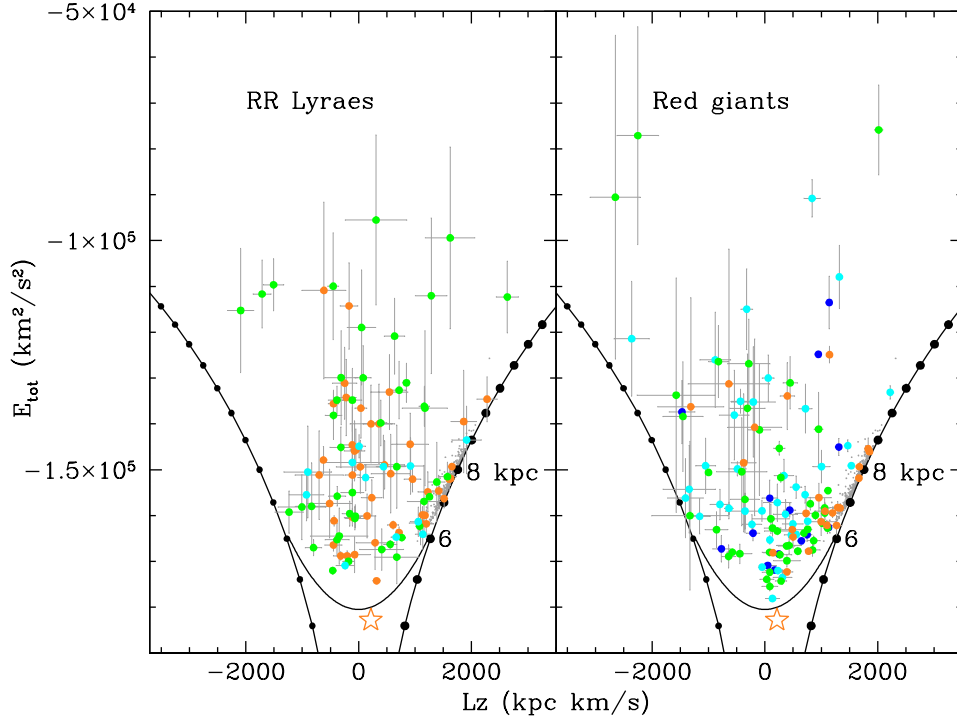


FIG. 7.— The energy-angular momentum diagram for our sample, showing RR Lyrae variables on the left and (first ascent) red giants on the right. Points are coded by metallicity as in Figure 2. Lines mark loci of circular orbits and apogalacticon 7 kpc, as in Figure 6. The orange star is the globular cluster M4, which has $[\text{Fe}/\text{H}] = -1.22$ (Kraft & Ivans 2003).

branch morphology in the solar neighborhood is very blue (Kinman et al. 1994), most of them will become BHB stars. Thus we see that the lower binding energy of our RR Lyraes is consistent with the result of Preston et al. (1991) that RR Lyraes have a shallower spatial distribution than BHB stars, and so are more likely to be found in the outer halo. Our RR Lyrae sample contains more objects from the outer halo than the red giant sample, although not all RR Lyraes in our sample are outer halo objects, as can be seen in Figure 8.

would suggest that these outer halo objects were also younger, as originally suggested by Searle & Zinn (1978) and then by Zinn (1993). The younger age of an accreted outer halo compared with the inner halo formed *in situ* makes sense in the light of the theoretical expectation that the first stars to form in the Galaxy would be in the rare high-density peaks, and would be centrally concentrated (Diemand et al. 2005); outer halo objects would form somewhat later. The dominance of retrograde orbits in the low binding-energy stars of both types is also interesting in the light of the discovery of Carollo et al. (2007) that the outer halo has retrograde rotation. It will be very interesting to see whether the nearby BHB stars (which may be older than the RR Lyraes) share the properties of the red giants in our sample in this diagram.

There are other interesting differences between the RR Lyrae and red giant kinematics in our sample: many of the more bound red giants are have prograde orbits, including a number close to the circular orbit line, while the RR Lyraes have a smoother distribution of orbital angular momenta.

2.5. Trends with Metallicity

Trends with metallicity are interesting because they give a handle on two processes: dissipational collapse with star formation subsequently enriching later generations, and dynamical friction, which is more effective for massive objects which produce stars with higher mean metallicity because of the mass-metallicity relation (eg Lee et al. 2006). We see an interesting difference in kinematics between the very metal-poor stars (with $[\text{Fe}/\text{H}] < -1.5$) and the metal-rich halo stars (with $-1.5 < [\text{Fe}/\text{H}] < -1.0$), in Figure 2, where stars with different metallicity are shown in different colors.

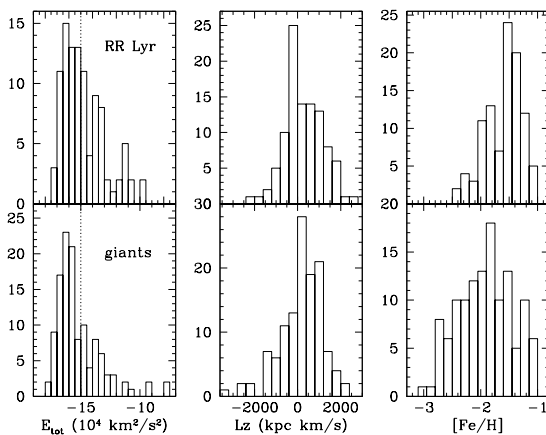


FIG. 8.— Histograms of E_{tot} , L_z and $[\text{Fe}/\text{H}]$ for the RR Lyrae and red giant subsamples. RHB stars have been omitted. The energy of the LSR orbit is shown on the left panels with a dotted line. It can be seen that the giants are more tightly bound on average than the RR Lyraes.

Connecting horizontal-branch morphology to age

While the entire sample has values of L_z ranging from -3000 to 2700 kpc km s^{-1} , there are no stars with intermediate metallicity ($-1.0 > [\text{Fe}/\text{H}] > -1.5$) which have L_z below -800 kpc km s^{-1} . (Note that with a median halo metallicity of -1.6 , eg Ryan & Norris 1991, , these intermediate-metallicity stars account for almost half of the halo, although they are under-represented in our sample because of the relative ease of identifying very metal-poor giant stars in surveys.)

We see the trend with metallicity more easily in the histograms of Figure 9. The median L_z value for the metal-rich stars is 545 kpc km s^{-1} , significantly higher than the median for the metal-poor stars (135 kpc km s^{-1}). The sample of Sommer-Larsen & Zhen (1990) also shows this difference in L_z for more metal-rich halo stars.

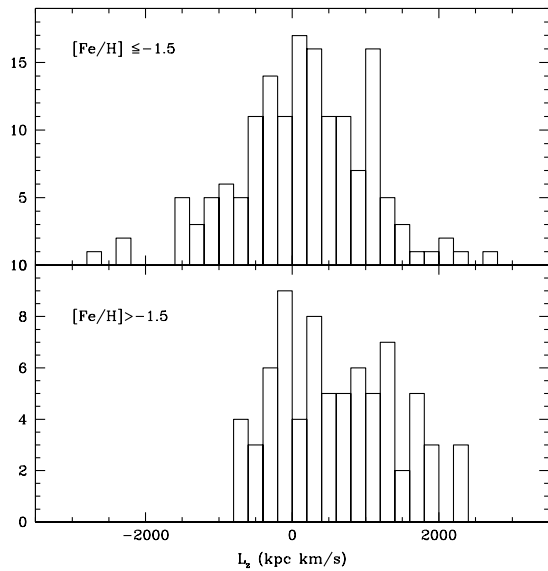


FIG. 9.— Histograms of L_z values for stars with L_\perp less than 1400 kpc km s^{-1} . Upper panel shows stars with $[\text{Fe}/\text{H}] < -1.5$, lower panel those with $[\text{Fe}/\text{H}]$ between -1.0 and -1.5 .

3. DISCUSSION

3.1. Halo flattening: another component

The first suggestions that the halo's flattening might be variable with radius were in the 1950s and 60s by Schmidt (1956) and Kinman et al. (1965), studying globular clusters and RR Lyraes respectively. While both studies were contaminated by some metal-rich objects, it is unlikely that this was the only reason for their findings. Hartwick (1987) suggested a two-component halo based on RR Lyrae samples. Zinn (1993) also found a two-component halo by studying the kinematics, space distribution, metallicity and ages of globular clusters in the Galaxy. The Old Halo clusters of the inner halo show a flattened distribution and have some rotation (although much less than the disk's). The Younger Halo is spherical and has no net rotation. More recently, Miceli et al. (2008) discussed a two-component halo with distinct radial distributions for different Oosterhoof types in their large sample of RR Lyraes, and Carollo et al. (2007) used a very large sample of halo stars from the SDSS survey to extend the description of the two-component halo. Of

particular importance to an understanding of the population characteristics of the two components is Carollo et al's demonstration that the near-spherical outer halo has a net retrograde rotation and that it is more metal-poor than the flattened inner halo.

All of the field star results are for relatively distant samples. What of samples like our own, with many stars less than 1 kpc from the plane? Sommer-Larsen & Zhen (1990) used an early local sample of 151 metal-poor, predominantly giant and RR Lyrae stars with less accurate data than ours. Using only stars with $[\text{Fe}/\text{H}] < -1.5$, they reconstructed the density distribution of the halo, found that these metal-poor stars had a two-component structure, and noted that their flattened shape was due to velocity anisotropy, not rotation. While they do not explicitly quote the axial ratio of the flattened component, it can be seen in their Figure 6 that it is quite flat: c/a around 0.25 . In general, our analysis agrees well with these early results. Sommer-Larsen & Zhen (1990) suggested that either the metal-poor stars in the flattened component formed in an anisotropic, dissipative collapse (with the anisotropic infall caused by a flattened dark halo) or by late infall of metal-poor gas clouds which “plunged into the disk” and formed stars there.

Preston et al. (1991) used BHB stars and RR Lyraes (which were dominated by stars more than 2 kpc from the plane except for some very close to the galactic center) and derived a density law for the halo which became more spherical with increasing radius, with axial ratio $c/a = 0.5$ at the galactic center. However, when they used this model to predict the RR Lyrae density near the Sun, they found that it under-predicted the known value by a factor of two, concluding that “there exists a metal-poor population, confined to a volume near the galactic plane, which has remained undetected in intermediate and high-latitude surveys.” It seems very likely that Preston et al were describing what we call the low L_\perp component of the halo. Green & Morrison (1993) also suggested the existence of this highly flattened halo component using a sample of BHB stars within 500 pc of the Sun.

Thus there are *two* flattened components in the inner halo: the moderately flattened, $c/a \sim 0.6$ component identified by Kinman et al. (1965), Hartwick (1987), Preston et al. (1991), Zinn (1993) and Kinman et al. (1994) from more distant samples of halo stars, and the highly flattened, $c/a \sim 0.2$ component foreshadowed by Sommer-Larsen & Zhen (1990), Preston et al. (1991) and Green & Morrison (1993) and revealed in more detail in this work. We will discuss possible origins for these two components below.

Chiba & Yoshii (1998) and Chiba & Beers (2000) also studied local samples, although the one used by the latter (the sample of Beers et al. 2000) suffered from large distance errors for a number of stars (see Section 2.1 and Kepley et al. 2007). Chiba & Yoshii (1998) focused their attention on quantifying the contribution of the metal weak thick disk to their sample. Curiously, although Chiba & Beers (2000) use a local sample, they conclude that their results are similar to those of the more distant samples such as Preston et al. (1991): a halo with an axial ratio decreasing as R decreases and only moderate flattening in the center. We suggest that the large distance errors of some of the stars in their sample might have made it difficult to distinguish between a moder-

ately flattened and a highly flattened inner halo. We explored the effects of a larger measurement error using our data, by adding a random number picked from a Gaussian with twice the error in L_z and L_\perp to each datapoint. Much of the structure that we see is no longer visible, showing that our careful sample selection was needed.

Recently, Brown et al. (2008) have presented a preliminary kinematic analysis of a large sample of 2414 BHB stars with distances larger than 2 kpc from the galactic plane. They find a flattened component, but identify it with the metal-weak thick disk because of its significant rotation. However, in their paper they simply solve for mean rotation of the entire sample as a function of distance from the plane, and find both a trend with z and a surprisingly large random variation in mean rotation (from $+150$ to -60 km s $^{-1}$) over the range of z heights covered by their sample. Kinman et al. (2008) have shown, using proper motion information for the most nearby stars in this sample, plus another sample of nearby BHB stars, that the mean rotation of BHB stars close to the plane is close to zero. Thus the flattened component in the Brown et al. (2008) sample is likely to be associated with our low L_\perp group.

It is also interesting to note that the nearest globular cluster, M4, has properties consistent with membership in the highly flattened halo. Using the data given in Dinescu et al. (1999) we find that it has $z = -0.5$ kpc, $L_z = 215 \pm 141$ kpc km s $^{-1}$ and $L_\perp = 32 \pm 22$ kpc km s $^{-1}$. We show its position in the energy and angular momentum diagrams of Figures 2 and 6 with an open 5-pointed star. Using the data from Dinescu et al. (1999) and Casetti-Dinescu et al. (2007), we find that there are another four globular clusters with R_{gc} between 6 and 10 kpc which have similar orbital properties to our low L_\perp group: NGC 4372, 4833, 5139 (ω Centauri) and 6779, and another four with R_{gc} less than 6 kpc: NGC 5986, 6093, 6656 and 6712.

3.2. The thick disk

It is remarkable how little contribution the thick disk makes to our sample; the region of the L_z - L_\perp diagram occupied by the Nordström et al. (2004) local dwarfs, a sample almost totally dominated by the disk, contains less than 5% of our sample. Given the fact that thick disk stars outnumber halo stars by 1–2 orders of magnitude in our region, this could put strong constraints on the size of the low-metallicity tail of the thick disk metallicity distribution. Earlier claims of a significant low-metallicity tail (Morrison et al. 1990) were over-estimates because of problems with the DDO metallicity calibration (Twarog & Anthony-Twarog 1994, Ryan & Lambert 1995, Chiba & Yoshii 1998).

However, both the RR Lyrae and the red giant/RHB samples are seriously incomplete at low latitudes, as can be seen in Figure 10. This incompleteness would reduce the number of thick disk stars found in our sample. While this is unlikely to be a strong effect for our very local sample (recall that the mean distance of our stars is 1 kpc), we cannot use this sample to obtain an unbiased estimate of the density of metal-weak thick disk stars unless we engage in complex corrections for our selection effects. By contrast, the sample of Norris et al. (1985) which was used for first studies of the metal-weak thick disk

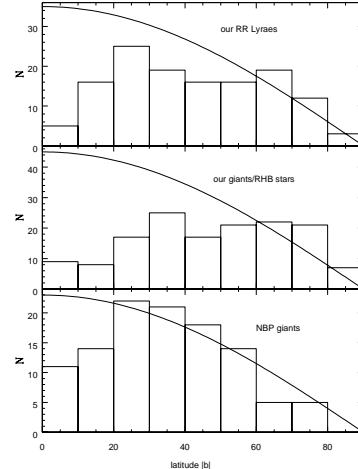


FIG. 10.— Histograms of latitude $|b|$ for (top) the RR Lyraes in our sample (middle) the red giants and RHB stars in our sample, and (bottom) the giants of Norris et al. (1985). The curve on each plot is $\cos(b)$. It can be seen by comparison with the curve on each plot that our local sample has serious incompleteness at low latitude, and the NBP sample is much more complete.

(Norris et al. 1985, Morrison et al. 1990) shows much less incompleteness with latitude, as can be seen in the bottom panel of Figure 6. An upcoming analysis of the metallicity of the stars in this sample (Beers, private communication, Krugler et al. 2004) would be the best way to obtain an unbiased estimate of the local density of the metal-weak thick disk.

3.3. Summary of Results

Pulling together all of the above analysis, we have the following results.

(1) We find evidence for an additional component to the inner halo, which is highly flattened ($c/a \sim 0.2$), pressure-supported and has a small prograde rotation. This component is not associated with the metal-weak thick disk, which is predominantly rotationally supported. The new component shows a smooth distribution of L_z .

This component is separate from the moderately flattened inner halo which was discovered using samples of halo stars located further than 1 kpc from the Sun, for example by Kinman et al. (1965), Hartwick (1987) and Preston et al. (1991). This moderately flattened component has axial ratio (c/a) of ~ 0.6 . If the globular clusters are representative of the field stars in this moderately flattened component, it is predominantly old and also has a small prograde rotation. Carollo et al. (2007) also ascribe a “modest prograde rotation” to their moderately flattened inner halo.

The highly flattened component forms about 40% of our sample. However, this could be an under-estimate of its true density as the samples on which we base our analysis avoid low latitudes (see Figure 10).

(2) The remaining 60% of stars in our sample, whose orbits reach further from the plane, have a mean rotation close to zero and a clumpy distribution in angular momentum and energy.

(3) We see trends with metallicity. The low metallicity stars in our sample ($[\text{Fe}/\text{H}] < -1.5$) show a mean rotation near zero and a clumpy distribution in energy and

angular momentum.

The intermediate-metallicity stars ($-1.5 < [\text{Fe}/\text{H}] < -1.0$) cover the whole range of L_{\perp} (in other words, they belong both to the highly flattened component and to the other(s)), but there is a higher proportion of these intermediate-metallicity stars in the low L_{\perp} region. The intermediate-metallicity stars have a small prograde rotation and a clumpy distribution in angular momentum and energy.

(4) The RR Lyrae variables in our sample have a lower binding energy, on average, than the red giants, with half of the RR Lyraes being less tightly bound than the LSR orbit, in contrast to the red giants where only one third of the stars are less tightly bound. Because the local horizontal branch morphology is very blue, this suggests that the younger RR Lyrae stars are less strongly bound to the Galaxy. The RR Lyrae sample also appears to contain more stars on retrograde orbits.

4. FORMATION AND EVOLUTION OF THE INNER HALO

We will now discuss the different stages of halo formation and the constraints placed on various theories by our data. In particular we will examine possible formation paths for the highly flattened halo component which is supported by velocity anisotropy.

4.1. The First Halo Stars

Theory predicts that the first stars to form in the Galaxy's halo occupy dark halos which formed from very rare high-density peaks in the primordial density field. At this early stage (perhaps beginning earlier than $z=10$, less than 0.5 Gyr after the Big Bang) the Galaxy's disk had not formed. Diemand et al. (2005) use simulations to predict that the density distribution of such stars is more centrally concentrated than the rest of the halo. Many of these first stars will now be found in the inner few kpc of the Galaxy; however there will still be a few with orbits that reach the solar neighborhood.

How might we identify these first stars? We would expect the very first stars to have extremely low metallicity. However, the amount of chemical enrichment that occurs in the earliest star formation in the halo is not well constrained, so we do not know whether only extremely metal-poor stars were formed at this stage, or whether some stars closer to typical halo metallicities were also formed. We see no unique pattern in the angular momentum or energy distribution of the most metal-poor stars in our sample. We plan to extend our sample to stars of extremely low metal abundance and check whether their kinematics are different.

Where would the early halo stars, formed long before the disk, appear in the L_z - L_{\perp} diagram? We would expect them to have low total energy (be tightly bound to the Galaxy) and have both low L and low L_z . Interestingly, the very metal-poor star CD-38 245 ($[\text{Fe}/\text{H}]=-4.0$) is in the original sample of Anthony-Twarog & Twarog (1994) but was excluded from our sample because of its distance (3.3 kpc). However, its angular momentum and energy are well-determined, and fit the expectation for a star formed very early: $L_z = -110 \text{ kpc km s}^{-1}$, $L_{\perp} = 254 \text{ kpc km s}^{-1}$ and $E_{\text{tot}} = -1.6 \times 10^5 \text{ km}^2 \text{ s}^{-2}$: it is on a near-radial orbit, confined to the inner halo. It is quite possible that CD-38° 245 was formed early, and is a genuine "original inhabitant" of the inner halo.

Because the Galaxy itself is quite small at such early times, the first halo stars to form would have low total angular momentum, and thus low L_{\perp} . However, they cannot form our entire low L_{\perp} group, because of its large range in L_z . Also, it is unlikely that the chaotic conditions under which the first stars formed would allow a very flattened configuration, such as this group, to survive. This is also the reason why any disk which formed during the early period where the Galaxy's halo was growing via violent merging would not survive.

We should note, however, that there is another evolutionary path which will also produce stars with low angular momentum and energy: dynamical friction dragging satellites in from the outer halo. So the possession of low angular momentum and low energy are not sufficient to identify early halo stars.

4.2. Accretion and halo growth before disk formation

4.2.1. Substructure in E and L

Before the disk forms, mergers will cause the Galaxy's gravitational potential to vary strongly. This violent relaxation might smooth out any dynamical record of the origins of stars formed then, and lead to a kinematically smooth distribution. This has been the source of a general expectation that the inner halo be smoother than the outer halo. However, in our inner halo sample, the only stars which display a smooth L_z distribution are ones which occupy the highly flattened component. We have argued above that we would not expect this component to be formed before the disk because such a flattened spatial distribution would be destroyed by mergers. Thus its smoothness cannot be ascribed to violent relaxation and is not relevant here.

However, we would expect many of the stars in the remainder of the sample to be formed at this stage of the halo's growth, and we see no evidence for a complete smoothing of kinematical quantities by violent relaxation there. We are not aware of any other observational study which finds such a clumpy distribution in energy and angular momentum. We suggest that the larger distance errors of previous samples (which become magnified when quantities such as energy and angular momentum are measured) have obscured the intrinsic clumpiness of the data there. We note that our clumpy distribution in angular momentum and energy does not contradict the result of Gould (2003) that no more than 5% of the local halo comes from a given stream because multiple streams can come from a single progenitor. Results from simulations of the dark halo (Helmi et al. 2002; 2003, Diemand et al. 2005; 2007) have a similar result: the velocity distribution of the dark matter is quite smooth there, despite a small number of progenitors supplying the field stars of the inner halo.

The clumpy distribution in energy and angular momentum implies that either the violent relaxation was not violent enough to destroy structure in angular momentum and energy, or this process was limited to the inner few kpc of the Galaxy, and did not reach the solar neighborhood. This is good news for galactic archaeology, as it will allow us to trace various halo substructures to very early times. If, in addition to the preservation of some initial conditions through the violent relaxation stage, a small number of accreted objects formed most of

the stars in the inner halo, as suggested by the simulations of Helmi et al. (2002) and Helmi et al. (2003), this would give a natural explanation for the clumpiness we see. It is unlikely that such a clumpy distribution in angular momentum would be produced by a large number of progenitors with distinct orbital properties.

4.3. Pure accretion

The corollary of the expectation that the earliest stars will form in the high-density peaks near the center of the Galaxy is that star formation in the lower-density regions that join the Galaxy as its halo grows should start somewhat later. This leads to the expectation that RR Lyrae samples, which should be younger on average than BHB samples, should be less strongly bound to the Milky Way. We have discussed the fact that we see this in our sample in Section 2.4.

Now let us focus on “pure” accretion, unassisted by dynamical friction, which builds up the outer halo, and ask whether any of these outer halo objects would be found in our local sample. As the Galaxy grows, and its turnaround radius (where objects separate from the Hubble flow and become bound to the Galaxy) increases, it becomes harder for accreted objects to reach the solar neighborhood unless they are on near-radial orbits. However, radial orbits are quite common for infalling satellites: Benson (2005) shows that more than half of the orbits of satellites in the simulations he studies have eccentricity between 0.9 and 1.0 when they enter their host halo, showing that this is not an impossible requirement⁹.

Such objects, with near-radial orbits, have all components of angular momentum near zero. If dynamical friction has not occurred, then we have the additional diagnostic that the orbits will have low binding energy (high total energy) as well, since they fell into the Galaxy from a large distance. Stars from these late-accreted small objects will be found in the region near $L_z \sim 0$ and E_{tot} greater than, say, $-1.4 \times 10^5 \text{ km}^2 \text{ sec}^{-2}$. Intriguingly, there is a preference for slightly retrograde orbits in this region of the L_z - E_{tot} diagram, and we see more of this component in the (possibly younger) RR Lyrae sample than in the red giants. This may be related to the result of Carollo et al. (2007) that the outer halo has a small net retrograde motion; if the material which was added to the Milky Way at later times had a different mean angular momentum from the material which formed the disk, then the only part of this outer halo that could reach the solar neighborhood without help from dynamical friction would be the stars on near-radial orbits. The remainder of these stars would then populate the outer halo. However, it must be remembered that dynamical friction can also populate this area, and in fact many of these stars have also been claimed to be the debris of ω Cen’s progenitor (Dinescu 2002, Brook et al. 2003, Meza et al. 2005).

We have noted that it is not likely that our highly flattened halo component formed before the disk because the ongoing mergers which only stopped when the present-day disk formed would tend to heat this very flattened component. However, the *moderately* flattened

inner halo could have been formed during mergers of gas-rich infalling objects at early times, in a number of ways. For example, when gas-rich infalling objects merge, the gas is likely to form stars with low net angular momentum. This process is referred to as “dissipative merging” by Bekki & Chiba (2001) and seen (to excess) in early cosmologically-based galaxy formation simulations such as that of Navarro et al. (1995). Stars formed in this way would likely have low metallicity and make up part of the inner halo, although the gas might have experienced some pre-enrichment. Bekki & Chiba (2001) use this process to explain the moderately-flattened, somewhat metal-enriched inner halo.

4.4. Dynamical Friction

There is another way for an accreted satellite to sink to the inner halo, even without a radial orbit. Dynamical friction is a purely gravitational process, caused by the formation of a gravitational wake as a massive object travels through a density field. It allows satellites, given sufficient mass and time before disruption, to transfer energy and angular momentum to the dark halo and sink toward the galactic center and the disk plane. Dynamical friction from the halo will permit massive satellites which are accreted at a later time to end up in the inner halo, even if their initial perigalactica are large. The efficiency of dynamical friction is a strong function of the mass ratio between object and host. In the case of a single host, it varies strongly with the satellite mass (M^2 ; Binney & Tremaine 1987); see also Figure 13 of Walker et al. (1996), so we would expect the more massive objects (which are also likely to form more metal-rich stars: Mateo 1998, Tremonti et al. 2004, Lee et al. 2006, Erb et al. 2006) to be more successful in reaching the solar neighborhood via this process.

The strong dependence of dynamical friction on the mass of the accreted object is important for the inner halo: it means that it will be dominated by debris from only a few relatively massive satellites (Helmi et al. 2002; 2003), and may well be related to the clumpiness we see in E and L. Meza et al. (2005) present simulations to show that the disruption of a single satellite via dynamical friction can in fact lead to a number of long-lived groupings in energy and angular momentum space.

Dynamical friction can also affect the spatial distribution of the inner halo, as follows. Theory predicts that only a few progenitors contributed most of the mass of the inner halo, making it less likely that the result of these few accretions will be exactly spherical. Accretion of hundreds of smaller sub-halos will likely produce a spherical outer halo, while it would not be surprising if the stars stripped from the few massive objects which formed the inner halo produced a somewhat flattened inner stellar halo. So the cosmological predictions for the growth of the dark halo will quite naturally produce a moderately flattened inner halo and a near-spherical outer halo.

4.5. Disk Formation

As we have noted above, the Galaxy’s potential needs to settle down (the epoch of major mergers needs to end) before we can form either the dynamically cold thin disk or our highly flattened halo component, since they would

⁹ Benson (2005) cautions that larger studies are needed to disentangle the effects of redshift and mass on this quantity.

be destroyed by these violent variations in the gravitational potential. The need for angular momentum conservation in producing the large disks that we see today also requires this. While the classical picture of smooth gas dissipation and infall conserves angular momentum, mergers between gas-rich objects at early times can transfer both energy and angular momentum to the dark halo (eg Navarro et al. 1995). Angular momentum will not be conserved during this process, which dominates at early times, unless feedback processes keep gas out of the cores of the merging objects. This was first suggested by Navarro et al. (1995); we will see below that recent simulations have confirmed the result.

Galaxy formation simulations cannot trace star formation in detail because the spatial resolution needed far exceeds what is computationally possible when studying an entire galaxy. Thus average prescriptions are used to model the complex, multi-phase gas physics. In many of the early simulations of galaxy formation, the angular momentum of the gas was not conserved: gas cooled, collapsed and formed stars early, and then mergers transferred its angular momentum to the dark halo (eg Steinmetz & Muller 1995, Abadi et al. 2003) and only small disks were formed (the “angular momentum problem”). Recent simulations which include a more complex treatment of feedback (eg Springel & Hernquist 2003) have formed larger, more realistic late-type disks (Robertson et al. 2006, Zavala et al. 2008, Governato et al. 2007). Because the accretion of a large satellite will destroy a dynamically cold stellar disk, the present-day disk starts to form only after major mergers have ceased. However, the star formation rate in the disks formed in even the most recent studies tends to peak at early times, soon after the last merger (see, for example, Abadi et al. 2003, Governato et al. 2007), in contrast to the star formation rate in the Milky Way disk, which is thought to have been roughly constant for most of its life (Twarog 1980, Rocha-Pinto et al. 2000). More work on modelling feedback and gas flows is clearly needed before the major properties of late-type disks are reproduced.

In the simulations of Abadi et al. (2003) and Springel & Hernquist (2005), the last major mergers before disk formation were between gas-rich galaxies. It is possible that one or both of the halo’s flattened components were created in a way that was intimately related to the formation of the disk. In these simulations, the stars which were already part of the galaxies in the last major mergers formed a flattened component, and gas from these merging objects then settled into a thin disk and formed stars. (It is not clear at this stage whether the flattened component formed from accreted stars is caused by the specific initial conditions of these simulations or whether it is a general outcome.) Abadi et al. (2003b) identify this flattened component (despite its rather large scale height of 2.7 kpc) with the thick disk, which has a scale height of ~ 1 kpc in the Milky Way (Reylé & Robin 2001, Ng et al. 1997) and note that it has kinematics “intermediate between halo and disk”: the stars have a mean rotation of around 150 km s^{-1} but a large velocity dispersion. This moderately flattened component might also be related to the flattened inner halo first suggested by Kinman et al. (1965). As more simulations are published, it will be interesting to see the variation of scale

height and rotation of the components formed from the stars in the satellites which define the orientation of the disk.

It is also possible that the low L_{\perp} group was formed at this stage. The gas that came in with them could form stars in a flattened configuration that would form our low L_{\perp} group, instead of starting to form the disk. Which outcome occurs (rotationally supported disk or highly flattened halo) will depend on the angular momentum content of this gas. Since, by construction, the merger of these satellites was the last major one experienced by the Galaxy, any flattened stellar configuration formed after this time will not be subjected to huge variations in the Galaxy’s potential, and so it will be able to survive. This would explain the fact that the highly flattened component has stars which are more metal-rich than the overall halo, because stars from the galaxies which merged would have already polluted their ISM with some metals. While gas on predominantly radial orbits in an extremely flattened configuration (like the present-day young thin disk) will be likely to “self-cross” and shock, forming a more rotationally supported component, the low L_{\perp} group does not have such extreme flattening, so the gas carried in with the satellites which experience the last major mergers could still form the low L_{\perp} component.

The accretion and settling to the disk plane of gas and subsequent star formation will continue to build the thin disk in a process that continues to this day. Orbits of inner halo stars will be affected by the potential of this highly flattened disk, and could increase the flattening of the inner halo via adiabatic contraction, as originally pointed out by Binney & May (1986). Chiba & Beers (2001) have shown that this process is not sufficient to form an inner halo with axial ratio as high as 0.7; we have seen that the actual flattening of the inner halo is closer to 0.6. So adiabatic contraction alone is unlikely to form the moderately flattened inner halo.

4.6. *Fashionably late: after disk formation*

After the disk forms, we have another source of dynamical friction which can affect the orbits of objects which reach the inner Galaxy. Unlike dynamical friction with the halo, this process will be more efficient for objects on prograde orbits because the lower relative velocity of satellite and disk stars enhances the formation of the gravitational wake and so increases dynamical friction (Walker et al. 1996, Abadi et al. 2003, Meza et al. 2005). We would thus expect to see debris from objects which experience dynamical friction with the disk to tend to have a net prograde rotation. It is still possible for dynamical friction to bring objects on retrograde orbits into the inner Galaxy, but the process will be significantly slower. For example, Bekki & Freeman (2003) show how the angular momenta of stars in a possible progenitor of the retrograde, tightly bound globular cluster ω Centauri change as it is dragged down into the plane.

After the merger rate of the early Galaxy settles down and the disk forms at around $z=2$, the physical conditions are appropriate for the survival of our flattened (low L_{\perp}) group. As time goes on, the turnaround radius continues to grow, and, as noted above, it becomes steadily more difficult for objects to reach the inner halo without the help of dynamical friction. Satellites on ex-

tremely radial orbits can still do so, but will not form our low L_{\perp} component because it has quite a range in L_z . So, dynamical friction is an important part of the origin of this component. This fits in well with the result shown in Figure 9: more massive objects will also form more metal-rich stars on average, so this gives a natural explanation of the higher metallicity of this component.

Can we constrain the number of progenitors whose accretion formed this highly flattened component? The stars in this component have quite a large range of energy and L_z , although their L_{\perp} range is small. The energy and angular momenta of stars lost from a satellite will be determined by both the orbital energy and angular momentum of the satellite itself, and the position of the stars in the Galaxy when they are stripped. If the disruption happens within a few kpc of the Galaxy’s center, the satellite’s finite physical size will ensure that stars will gain different amounts of potential energy and angular momentum depending on their distance to the center when they are stripped from the satellite. Thus it is possible that even a single progenitor produced this component, if it was disrupted close to the Galaxy’s center. It is also possible that more than one satellite was disrupted to form it.

The formation of the disk will flatten the inner Galaxy’s potential, making it easier for dynamical friction with the halo to drag objects down into the plane. There are now two options: first that the satellite(s) were disrupted before they had a chance to experience dynamical friction with the disk or thick disk; and second that they were disrupted later, in which case dynamical friction with both halo and disk would have occurred. If only dynamical friction with the halo occurred, then the slightly prograde rotation of the highly flattened component is simply a coincidence. This would be easier to explain with one or a few progenitors.

If dynamical friction with the disk itself occurred, we have a “built-in” explanation for the small prograde rotation of this component. Dynamical friction with the disk is more efficient for objects on prograde orbits, since they will spend more time near the gravitational influence of the disk stars. In this case we would expect there to be a difference in $\langle L_z \rangle$ between objects with low L_{\perp} which experienced dynamical friction with the disk, and those whose orbits do not spend enough time close to the plane to experience disk dynamical friction, and so would be found with higher L_{\perp} .

At what distance above the plane does dynamical friction from the disk become important? We can produce a rough estimate for the current epoch by calculating where the density of the present-day thin disk and dark halo are roughly equal in the solar neighborhood. Using a simple isothermal halo with $V_c = 220 \text{ km s}^{-1}$ and $r_c = 2 \text{ kpc}$ and assuming a thin disk stellar density of $0.1 M_{\odot} \text{ per pc}^3$ we find that the densities are roughly equal at 2.3 thin disk scale heights ($z = 800 \text{ pc}$) So we would expect stars to need to spend significant time within 1 kpc of the plane in order to feel dynamical friction from the disk. This is quite interesting in the light of the $L_{\perp} = 350$ result, which is equivalent to a population scale height similar to the thick disk’s.

Why should dynamical friction produce a **smoother** distribution for stars close to the plane? The more massive satellites would have a larger stellar velocity dis-

person, but they will also produce more streams, which would need velocity accuracy of order 1 km s^{-1} to separate. If there was a single progenitor, the range of potential energy and angular momentum imparted to stars as they were stripped at different galactocentric radii would likely produce such a smooth distribution. It is more difficult to explain this smoothness in the case of a larger number of progenitors.

Another possibility is that the halo star orbits with low L_{\perp} are close enough to the plane to feel the effect of inhomogeneities in the disk potential due to spiral arms, giant molecular clouds and the bar. Scattering and heating caused by interactions with these massive objects would smooth the velocity distribution of the stars. However, the non-circular orbits of these halo stars ensure that the stars would not linger long within the gravitational reach of these large density inhomogeneities.

The origin of this low L_{\perp} group from processes involving dynamical friction makes the nine globular clusters with extended horizontal branches and orbits similar to the low L_{\perp} stars particularly interesting. Lee et al. (2007) suggest that the clusters with extended horizontal branches also have helium-enhanced second-generation subpopulations (which are directly observed in several cases, notably in ω Centauri). If the clusters were originally cores of ancient dwarf galaxies which have since disrupted (Bekki & Freeman 2003, Bekki & Norris 2006), and the galaxies were sufficiently massive to be affected by dynamical friction, then it would not be surprising to find them well represented in our low L_{\perp} group. In fact, five out of the six most tightly bound clusters with these orbital properties have extended horizontal branches, so their orbital properties are consistent with their origins as cores of ancient dwarfs.

In summary, we feel that late accretion, and dynamical friction with the dark matter halo (and perhaps also existing disk and thick disk stars) is the best way to explain the origin of the highly flattened inner halo.

5. SUMMARY

Using our sample of metal-poor giants, RHB stars and RR Lyraes, we find that the metal-poor halo has a highly flattened component, with axial ratio $c/a \sim 0.2$, a similar scale height to the thick disk, in the neighborhood of the Sun. This component was suggested by Sommer-Larsen & Zhen (1990) and predicted by Preston et al. (1991) and Green & Morrison (1993). The highly flattened component has a small prograde rotation, but most of its stars are on fairly eccentric orbits; this small rotation does not affect its flattening significantly. Stars of only moderate metal deficiency ($-1.5 < [\text{Fe}/\text{H}] < -1.0$) are more likely to be found in this component. This component is distinct from both the metal weak thick disk, which is primarily rotationally supported, and from the moderately flattened inner halo detected by many previous workers, which has a much less flattened density distribution.

We suggest that the most likely formation paths for this component would be “fashionably late” ones: either the stars formed from the gas accreted in satellites whose merger preceded the formation of the disk, or the stars were carried into the inner Galaxy by dynamical friction acting on their massive progenitor. Other formation paths such as dissipative mergers at early times

could have formed the moderately-flattened halo, but are unlikely to have formed our highly flattened component because the violent merging activity at these early epochs would have destroyed such a coherent component.

We find that the other stars in our sample, whose orbits reach further from the plane, exhibit quite a clumpy distribution in energy and angular momentum, suggesting that the chaotic conditions under which the early halo formed were not violent enough to erase the record of the conditions under which they were formed. Any truly smooth inner halo is either a very small component or only exists inside the solar neighborhood. This clumpy structure also suggests that only a small number of objects contributed the majority of stars to the inner halo, in line with theoretical expectations. It is possible that the progenitor galaxy of ω Centauri was one of these objects.

In addition we find that the RR Lyrae variables in our sample are somewhat less tightly bound to the Galaxy,

on average, than the red giants, and show a more retrograde rotation. This is consistent with earlier claims of a younger outer halo such as that of Searle & Zinn (1978) and Zinn (1993), with the retrograde outer halo of Carollo et al. (2007) and with the difference in kinematics between RR Lyrae and BHB stars at the NGP detected by Kinman et al. (2007).

6. ACKNOWLEDGEMENTS

AAK was supported by a NSF Graduate Research Fellowship during portions of this work; HLM by NSF grants AST-0098435 and AST-0607518; JS was supported by a grant from the NSF. AH acknowledges financial support from NOVA and NWO. HLM would like to thank Chris Mihos, Kathryn Johnston and James Bullock for useful discussions, Joanne Tidwell for suggesting the paper title, and Monty Python's Flying Circus for support.

REFERENCES

- Abadi, M. G., Navarro, J. F., Steinmetz, M., & Eke, V. R. 2003, *ApJ*, 597, 21
- Abadi, M. G., Navarro, J. F., Steinmetz, M., & Eke, V. R. 2003, *ApJ*, 597, 21
- Akaike, H., 1974, *IEEE Transactions on Automatic Control* 19, 716
- Anthony-Twarog, B. & Twarog, B. 1994, *AJ*, 107, 1577
- Beers, T., Chiba, M., Yoshii, Y., Platais, I., Hanson, R., Fuchs, B., & Rossi, S. 2000, *AJ*, 119, 2866
- Bekki, K., & Chiba, M. 2001, *ApJ*, 558, 666
- Bekki, K., & Freeman, K. C. 2003, *MNRAS*, 346, L11
- Bekki, K., & Norris, J. E. 2006, *ApJ*, 637, L109
- Benson, A. J. 2005, *MNRAS*, 358, 551
- Binney, J., & May, A. 1986, *MNRAS*, 218, 743
- Binney, J. & Tremaine, S. 1987, *Galactic Dynamics*, (Princeton, N.J.: Princeton University Press)
- Brook, C. B., Kawata, D., Gibson, B. K., & Flynn, C. 2003, *ApJ*, 585, L125
- Brook, C. B., Kawata, D., Scannapieco, E., Martel, H., & Gibson, B. K. 2007, *ApJ*, 661, 10
- Brown, W. R., Beers, T. C., Wilhelm, R., Allende Prieto, C., Geller, M. J., Kenyon, S. J., & Kurtz, M. J. 2008, *AJ*, 135, 564
- Carollo, D., et al. 2007, *Nature*, 450, 1020
- Casetti-Dinescu, D. I., Girard, T. M., Herrera, D., van Altena, W. F., López, C. E., & Castillo, D. J. 2007, *AJ*, 134, 195
- Chen, J. and Gupta, A. K. (2000), *Parametric Statistical Change Point Analysis*, Boston: Birkhäuser.
- Chiba, M., & Yoshii, Y. 1998, *AJ*, 115, 168
- Chiba, M., & Beers, T. C. 2000, *AJ*, 119, 2843
- Chiba, M., & Beers, T. C. 2001, *ApJ*, 549, 325
- Clewley, L., Warren, S. J., Hewett, P. C., Norris, J. E., Wilkinson, M. I., & Evans, N. W. 2005, *MNRAS*, 362, 349
- Csörgő, M. and Horváth, L. (1997), *Limit Theorems in Change-Point Analysis*, New York: John Wiley & Sons.
- Diemand, J., Madau, P., & Moore, B. 2005, *MNRAS*, 364, 367
- Diemand, J., Kuhlen, M., & Madau, P. 2007, *ApJ*, 667, 859
- Dinescu, D. I., Girard, T. M., & van Altena, W. F. 1999, *AJ*, 117, 1792
- Dinescu, D. I. 2002, ω Centauri, A Unique Window into Astrophysics, 265, 365
- Eggen, O. J. 1998, *AJ*, 115, 2397
- Erb, D. K., Shapley, A. E., Pettini, M., Steidel, C. C., Reddy, N. A., & Adelberger, K. L. 2006, *ApJ*, 644, 813
- Ganocy, S. (2003), "Estimation Problems from Data with Change Points," Ph.D Thesis, Department of Statistics, Case Western Reserve University. Adviser: Jiayang Sun
- Gould, A. 2003, *ApJ*, 592, L63
- Governato, F., Willman, B., Mayer, L., Brooks, A., Stinson, G., Valenzuela, O., Wadsley, J., & Quinn, T. 2007, *MNRAS*, 374, 1479
- Green, E. M., & Morrison, H. L. 1993, *The Globular Cluster-Galaxy Connection*, 48, 318
- Hartwick, F. D. A. 1987, *The Galaxy*, ed G. Gilmore and B. Carswell (Dordrecht, Reidel), 281
- Helmi, A. 2008, *Astronomy & Astrophysics Reviews*, in press
- Helmi, A., White, S. D. M., de Zeeuw, P. T., & Zhao, H. 1999, *Nature*, 402, 53
- Helmi, A., & de Zeeuw, P. T. 2000, *MNRAS*, 319, 657
- Helmi, A., White, S. D., & Springel, V. 2002, *Phys. Rev. D*, 66, 063502
- Helmi, A., White, S. D. M., & Springel, V. 2003, *MNRAS*, 339, 834
- Helmi, A., Navarro, J. F., Nordström, B., Holmberg, J., Abadi, M. G., & Steinmetz, M. 2006, *MNRAS*, 365, 1309
- Ishwaran, H., James, L. & Sun, J., 2001, *Journal of the American Statistical Association*, 96, 1316
- Johnston, K. V., Spergel, D. N., & Hernquist, L. 1995, *ApJ*, 451, 598
- Johnston, K. V., Hernquist, L., & Bolte, M. 1996, *ApJ*, 465, 278
- Jurcsik, J., Benkő, J. M., Bakos, G. Á., Szeidl, B., & Szabó, R. 2003, *ApJ*, 597, L49
- Kepley, A. A., et al. 2007, *AJ*, 134, 1579
- Kinman, T. D., Wirtanen, C. A., & Janes, K. A. 1965, *ApJS*, 11, 223
- Kinman, T. D., Suntzeff, N. B., & Kraft, R. P. 1994, *AJ*, 108, 1722
- Kinman, T. D., Cacciari, C., Bragaglia, A., Buzzoni, A., & Spagna, A. 2007, *MNRAS*, 375, 1381
- Kinman, T.D., Morrison, H.L. & Brown, W. 2008, submitted to the *Astronomical Journal*.
- Kraft, R. P., & Ivans, I. I. 2003, *PASP*, 115, 143
- Krugler, J. A., Frank, D., Beers, T. C., Norris, J. E., & Chiba, M. 2004, *Bulletin of the American Astronomical Society*, 36, 1377
- Lee, H., Skillman, E. D., Cannon, J. M., Jackson, D. C., Gehr, R. D., Polonski, E. F., & Woodward, C. E. 2006, *ApJ*, 647, 970
- Lee, J.-W., & Carney, B. W. 1999, *AJ*, 118, 1373
- Lee, Y.-W., Gim, H. B., & Casetti-Dinescu, D. I. 2007, *ApJ*, 661, L49
- Lynden-Bell, D., & Lynden-Bell, R. M. 1995, *MNRAS*, 275, 429
- Mateo, M. L. 1998, *ARA&A*, 36, 435
- Meza, A., Navarro, J. F., Abadi, M. G., & Steinmetz, M. 2005, *MNRAS*, 359, 93
- Miceli, A., et al. 2008, *ApJ*, 678, 865
- Morrison, H.L., Flynn, C., & Freeman, K.C. 1990, *AJ*, 100, 1191
- Navarro, J. F., Frenk, C. S., & White, S. D. M. 1995, *MNRAS*, 275, 56
- Navarro, J. F., Helmi, A., & Freeman, K. C. 2004, *ApJ*, 601, L43
- Ng, Y. K., Bertelli, G., Chiosi, C., & Bressan, A. 1997, *A&A*, 324, 65
- Nordström, B., et al. 2004, *A&A*, 418, 989
- Norris, J., Bessell, M. S., & Pickles, A. J. 1985, *ApJS*, 58, 463
- Preston, G. W., Shectman, S. A., & Beers, T. C. 1991, *ApJ*, 375, 121
- Reylé, C., & Robin, A. C. 2001, *A&A*, 373, 886

- Robertson, B., Bullock, J. S., Cox, T. J., Di Matteo, T., Hernquist, L., Springel, V., & Yoshida, N. 2006, *ApJ*, 645, 986
- Rocha-Pinto, H. J., Scalo, J., Maciel, W. J., & Flynn, C. 2000, *A&A*, 358, 869
- Ryan, S. G., & Norris, J. E. 1991, *AJ*, 101, 1865
- Ryan, S. G., & Lambert, D. L. 1995, *AJ*, 109, 2068
- Schmidt, M. 1956, *Bull. Astron. Inst. Netherlands*, 13, 15
- Schuster, W. J., Moitinho, A., Márquez, A., Parrao, L., & Covarrubias, E. 2006, *A&A*, 445, 939
- Schwartz G., 1978, *Annals of Statistics*, 6, 461.
- Schwarzschild, K. 1907, *Göttingen Nachr.*, p. 614.
- Searle, L., & Zinn, R. 1978, *ApJ*, 225, 357
- Sommer-Larsen, J., & Zhen, C. 1990, *MNRAS*, 242, 10
- Springel, V., & Hernquist, L. 2003, *MNRAS*, 339, 289
- Springel, V., & Hernquist, L. 2005, *ApJ*, 622, L9
- Steinmetz, M., & Muller, E. 1995, *MNRAS*, 276, 549
- Tremonti, C. A., et al. 2004, *ApJ*, 613, 898
- Twarog, B. A. 1980, *ApJ*, 242, 242
- Twarog, B. A., & Anthony-Twarog, B. J. 1994, *AJ*, 107, 1371
- Vivas, A. K., & Zinn, R. 2006, *AJ*, 132, 714
- Walker, I. R., Mihos, J. C., & Hernquist, L. 1996, *ApJ*, 460, 121
- Zavala, J., Okamoto, T., & Frenk, C. S. 2008, *MNRAS*, 387, 364
- Zinn, R. 1993, *The Globular Cluster-Galaxy Connection*, 48, 38